

Zfp148 Deficiency Causes Lung Maturation Defects and Lethality in Newborn Mice That Are Rescued by Deletion of p53 or Antioxidant Treatment

Volkan I. Sayin^{1,2}, Anna Nilton¹, Mohamed X. Ibrahim³, Pia Ågren¹, Erik Larsson^{1,2}, Marleen M. Petit^{1,2*}, Lillemor Mattsson Hultén¹, Marcus Ståhlman¹, Bengt R. Johansson², Martin O. Bergo³, Per Lindahl^{1,2*}

1 Wallenberg Laboratory, Institute of Medicine, The Sahlgrenska Academy at University of Gothenburg, Gothenburg, Sweden, **2** Department of Biochemistry, Institute of Biomedicine, The Sahlgrenska Academy at University of Gothenburg, Gothenburg, Sweden, **3** Sahlgrenska Cancer Center, Institute of Medicine, The Sahlgrenska Academy at University of Gothenburg, Gothenburg, Sweden

Abstract

The transcription factor Zfp148 (Zbp-89, BFCOL, BERP1, htβ) interacts physically with the tumor suppressor p53 and is implicated in cell cycle control, but the physiological role of Zfp148 remains unknown. Here we show that *Zfp148* deficiency leads to respiratory distress and lethality in newborn mice. *Zfp148* deficiency prevented structural maturation of the prenatal lung without affecting type II cell differentiation or surfactant production. BrdU analyses revealed that *Zfp148* deficiency caused proliferation arrest of pulmonary cells at E18.5–19.5. Similarly, *Zfp148*-deficient fibroblasts exhibited proliferative arrest that was dependent on p53, raising the possibility that cell stress is part of the underlying mechanism. Indeed, *Zfp148* deficiency lowered the threshold for activation of p53 under oxidative conditions. Moreover, both *in vivo* and cellular phenotypes were rescued on *Trp53^{+/-}* or *Trp53^{-/-}* backgrounds and by antioxidant treatment. Thus, *Zfp148* prevents respiratory distress and lethality in newborn mice by attenuating oxidative stress-dependent p53-activity during the saccular stage of lung development. Our results establish *Zfp148* as a novel player in mammalian lung maturation and demonstrate that *Zfp148* is critical for cell cycle progression *in vivo*.

Citation: Sayin VI, Nilton A, Ibrahim MX, Ågren P, Larsson E, et al. (2013) *Zfp148* Deficiency Causes Lung Maturation Defects and Lethality in Newborn Mice That Are Rescued by Deletion of p53 or Antioxidant Treatment. PLoS ONE 8(2): e55720. doi:10.1371/journal.pone.0055720

Editor: Sumitra Deb, Virginia Commonwealth University, United States of America

Received September 20, 2012; **Accepted** December 29, 2012; **Published** February 6, 2013

Copyright: © 2013 Sayin et al. This is an open-access article distributed under the terms of the Creative Commons Attribution License, which permits unrestricted use, distribution, and reproduction in any medium, provided the original author and source are credited.

Funding: The project was supported by the Swedish Research Council, Polysackaridforskning AB, the Swedish Cancer Foundation, the Swedish Heart-Lung Foundation, the University of Gothenburg, and by Lymphangiogenomics, an Integrated Project funded by the European Commission within its FP6 Program, under the thematic area "Life sciences, genomics and biotechnology for health" (contract no. LSHG-CT-2004-503573). The funders had no role in study design, data collection and analysis, decision to publish, or preparation of the manuscript.

Competing Interests: The authors have declared that no competing interests exist.

* E-mail: per.lindahl@wlab.gu.se

□ Current address: Laboratory for Molecular Oncology, Department of Human Genetics, K.U. Leuven, Leuven, Belgium

Introduction

Zinc finger protein 148 (*Zfp148*, Zbp-89, BFCOL, BERP1, htβ) is a krüppel type transcription factor that binds to GC-rich DNA sequences, thus activating or repressing transcription of target genes [1–8]. *Zfp148* targets represent a range of biological processes, however; the best characterized targets are associated with the cell cycle [5,6,8–10]. Those and other studies suggest a role for *Zfp148* in cell cycle control, but attempts to establish the *in vivo* function of the protein have met with limited success.

Zfp148 has been targeted three times in mice with inconsistent results [11–13]. Takeuchi reported that haploinsufficiency for *Zfp148* blocked germ cell differentiation in chimeric mice, thus precluding germline transmission of the targeted allele [13]. Another study suggested that *Zfp148*-deficient mice die at embryonic day (E) 9.5 with neural tube defects and anaemia [12]. Specific targeting of *Zfp148* exon 4, finally, caused postnatal lethality in homozygous mice and aggravated intestinal inflammation after dextran sulphate treatment [11]. Those discrepancies could reflect different targeting strategies, but the fact that all three papers report distinct phenotypes without apparent similarities

underscores that the physiological role of *Zfp148* remains poorly understood.

Cell culture experiments on the other hand strongly suggest that *Zfp148* is involved in cell cycle control [5,6,8,10,14,15]. For example, overexpressing *Zfp148* in cancer cells induces growth arrest or apoptosis by regulation of *Cdkn1a* (*p21*) and *Bak*, respectively, and silencing *Zfp148* induces senescence by regulation of *p16^{INK4a}* [5,6,8–10]. Moreover, *Zfp148* interacts with the tumour suppressor p53 and overexpression of *Zfp148* increases p53 levels in the nucleus [14]. In consistency with those reports, transgenic expression of *Zfp148* in intestinal epithelium induced apoptosis and reduced intestinal tumour formation in the APC^{Min/+} model of intestinal cancer [16]. The physiological relevance of this finding is, however, not clear since the protein was highly overexpressed.

In this study, we generate *Zfp148*-deficient mice and show that *Zfp148* plays an important and unexpected role in lung development. *Zfp148* maintains proliferation of pulmonary cells during the saccular stage of lung development by suppressing oxidative stress-dependent p53 activity, thus preventing respiratory distress and lethality in newborn mice. The results demon-

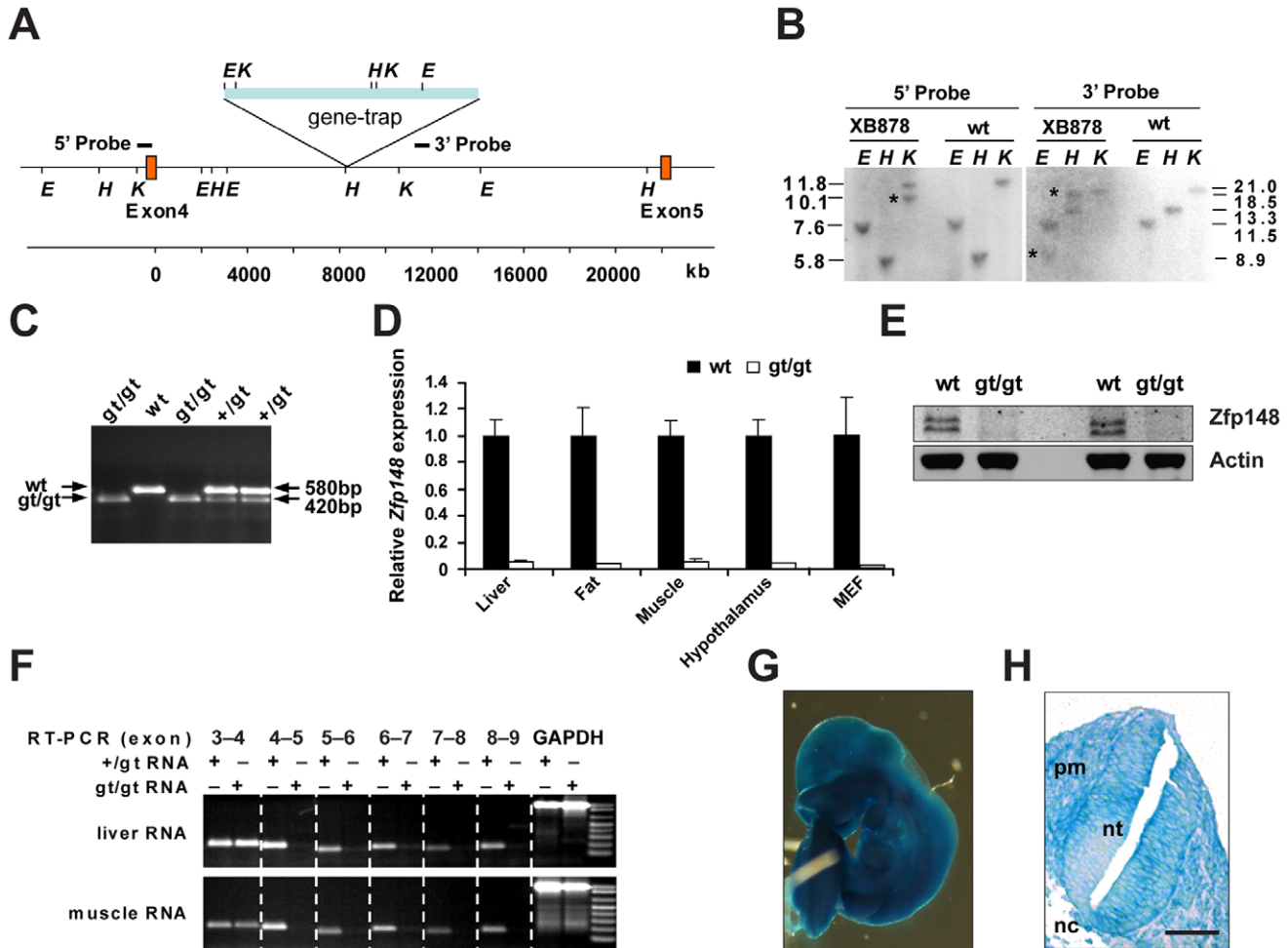


Figure 1. Generation of *Zfp148*^{gt/gt} mice. (A) Map of the *Zfp148* locus indicating the gene-trap insertion site, restriction sites for *EcoRI* (E), *HindIII* (H) and *KpnI* (K), and target sites for Southern blot probes. (B) Southern blot analyses of DNA from XB878 ES-cells and wild-type controls, digested with the restriction enzymes E, H, and K, respectively (asterisk indicates mutant band). Fragment size in kb. (C) PCR amplification across the gene-trap insertion on tail DNA from pups of *Zfp148*^{gt/gt} intercrosses confirmed gene-trap insertion at approximately 8500 base-pairs (bp) downstream of exon 4. The gene-trap specific band of 420 bp was amplified using a forward primer at 8256 bp downstream of exon 4 and a reverse primer in the gene-trap. The wild-type band of 580 bp was amplified using the same forward primer and a reverse primer at 8813 bp downstream of exon 4. (D) Real-time RT-PCR of the exon 4-5 border on cDNA from tissues of adult *Zfp148*^{gt/gt} and wild-type mice, respectively. (E) Western blots showing expression of *Zfp148* in *Zfp148*^{gt/gt} and wild-type mouse embryonic fibroblasts (MEFs). Actin was used as a loading control. (F) RT-PCR amplification across the indicated exon-exon borders of the *Zfp148* cDNA isolated from liver and muscle in *Zfp148*^{gt/gt} and *Zfp148*^{gt/gt} mice did not indicate cryptic splicing of the mRNA or alternative transcription start sites. Amplification of GAPDH was included as a loading control. (G) Whole mount image of X-Gal stained *Zfp148*^{gt/gt} mouse at E9.5. (H) Photomicrograph showing X-Gal stained transverse section of E9.5 *Zfp148*^{gt/gt} mouse. Scale bars, 100 μm. Neural tube (nt), notochord (nc) and paraxial mesoderm (pm).

doi:10.1371/journal.pone.0055720.g001

strate for the first time that *Zfp148* controls cell proliferation *in vivo*, in a p53-dependent manner.

Materials and Methods

Mice

All animal experiments were approved by the animal research ethics committee in Gothenburg, Sweden. *Zfp148*^{gt/gt} mice were generated from ES cell clone XB878 (BayGenomics) and maintained on a 129P2/OlaHsd and C57Bl/6 mixed genetic background. *Trip53^{tm1Tyj}* (*Trip53*^{+/+}) mice (The Jackson Laboratory) were maintained on a 129Sv and C57Bl/6 mixed genetic background. PCR primers used for genotyping are listed in Supporting Information Table S2.

Southern Blot Analysis

Genomic DNA was digested with *EcoRI*, *HindIII*, or *KpnI* and analyzed with a *Zfp148* intron 4-specific probe using standard protocols.

PCR Analyses

Primers are listed in Supporting Information Table S2.

Real-time Quantitative PCR

TaqMan and Sybr Green assays were performed as described [17] using TaqMan/Sybr Green universal PCR mastermix (Applied Biosystems) and the pre-designed TaqMan assays (Applied Biosystems) or RT-PCR primers listed in Supporting Information Table S2.

A**Zfp148 genotype distribution**

Stage / Genotype	wt (%)	+/gt (%)	gt/gt (%)	n
E9.5	30	43	27	77
E14.5–15.5	25	50	25	521
E18.5	25	49	26	220
P1	29	58	13	417
P9	34	54	12	82
P21	31	61	8	966

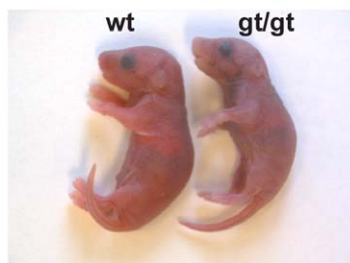
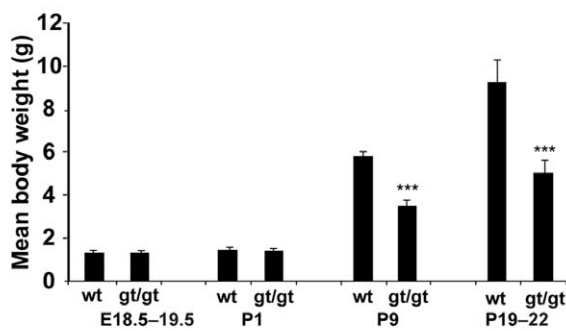
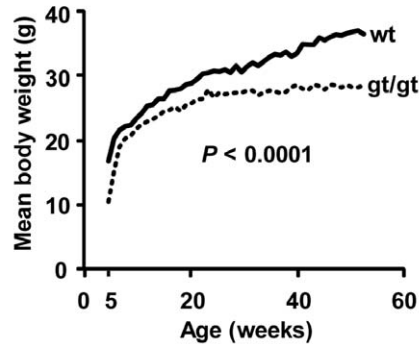
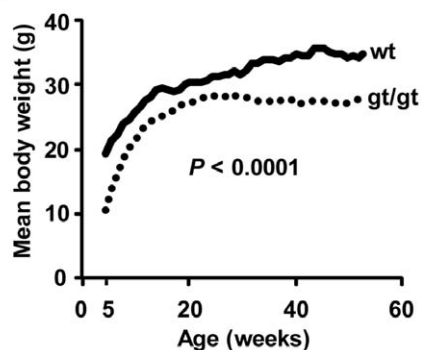
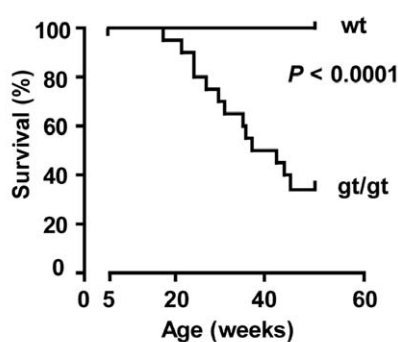
B**C****D****E****F**

Figure 2. Zfp148 deficiency causes lethality in newborn mice and growth retardation and reduced life span in adult mice. (A) *Zfp148* genotype distribution of offspring from heterozygous intercrosses. (B) Photograph of cyanotic *Zfp148^{gt/gt}* mouse and wt littermate at P1. (C) Body weight of wt, *Zfp148^{+/gt}* and *Zfp148^{gt/gt}* mice of mixed genders at E18.5–19.5 ($n = 12$ wt, 15 *Zfp148^{+/gt}*, 8 *Zfp148^{gt/gt}*), P1 ($n = 9$ wt, 13 *Zfp148^{+/gt}*, 7 *Zfp148^{gt/gt}*), P9 ($n = 28$ wt, 44 *Zfp148^{+/gt}*, 10 *Zfp148^{gt/gt}*) and P19–22 ($n = 10$ wt, 18 *Zfp148^{+/gt}*, 9 *Zfp148^{gt/gt}*). (D, E) Body weight curves for adult wt and *Zfp148^{gt/gt}* male (D) and female (E) mice, respectively ($n = 10$). (F) Kaplan-Meier plots showing survival of *Zfp148^{gt/gt}* and wt mice ($n = 20$). *** $P < 0.001$. doi:10.1371/journal.pone.0055720.g002

Western Blotting

Urea-dissolved total protein extracts were analyzed using antibodies recognizing Zfp148 (HPA001656), p16^{INK4a} (M-156, Santa Cruz Biotechnology), phospho-p53^{Ser18} (9284, Cell signalling Technology), and ACTIN (A2066, SigmaAldrich Atlas) as described [18].

X-Gal Staining

E9.5 embryos were dissected and immediately fixed at 4°C for 2 hours in 0.2% glutaraldehyde and 1.5% formaldehyde and whole-mount stained at 37°C overnight as in [19].

Immunohistochemistry

The primary antibodies anti-CC10 (Upstate Cell Signaling Solutions; 1:500) and anti-cleaved caspase 3 (9661, Cell Signaling; 1:750) were used for immunofluorescence and visualized with anti-rabbit IgG horseradish peroxidase-linked antibody (GE Healthcare; 1:200), TSA Cyanine 3 System (PerkinElmer) or goat anti-rabbit Alexa 546 (Molecular Probes; 1:500) in a Leica TCS SP5 confocal microscope or a Leica Image1 microscope (Leica Microsystems AG). BrdU positive cells were detected with 5-Bromo-2'-deoxy-uridine Labeling and Detection Kit I (Roche). Image analyses were done with BioPix iQ software (version 2.1.8., BioPix).

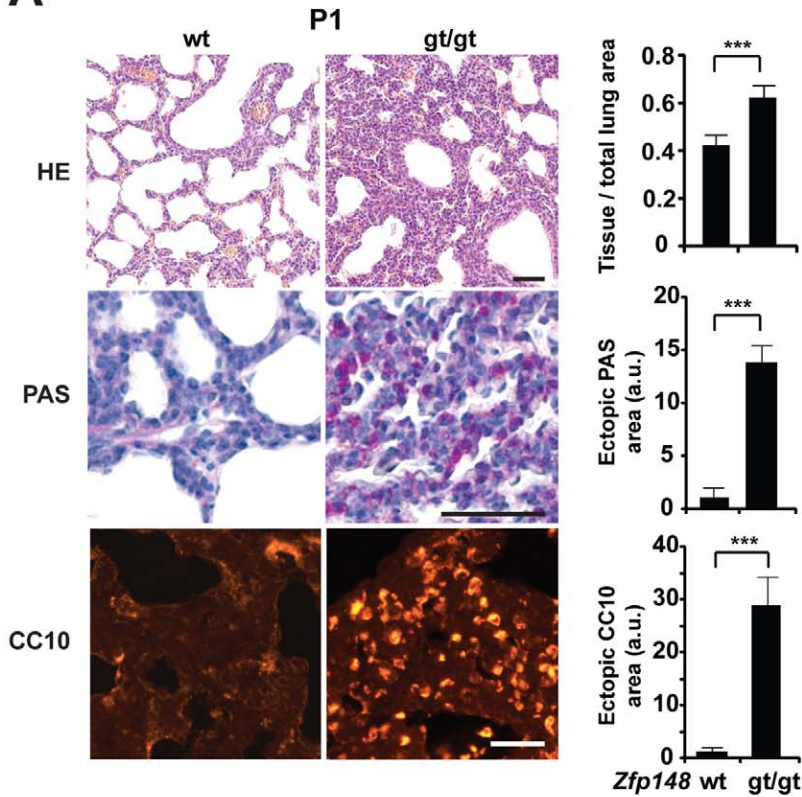
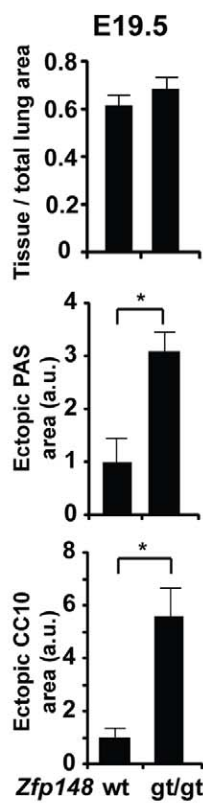
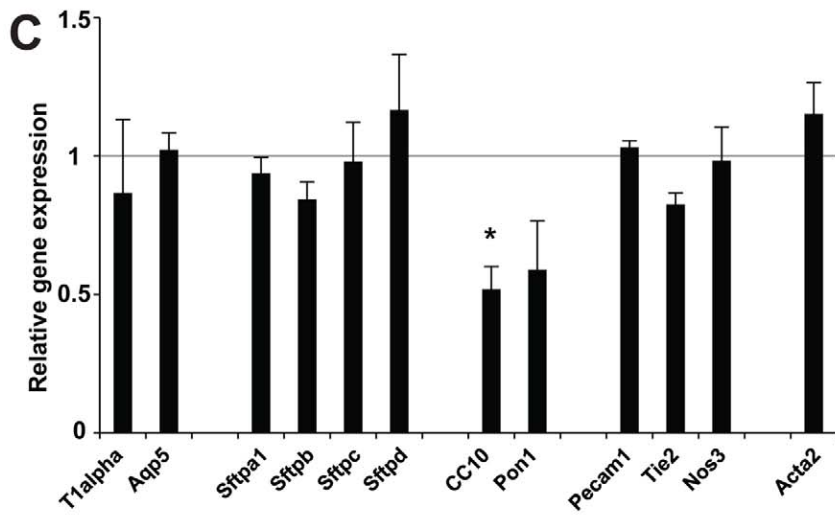
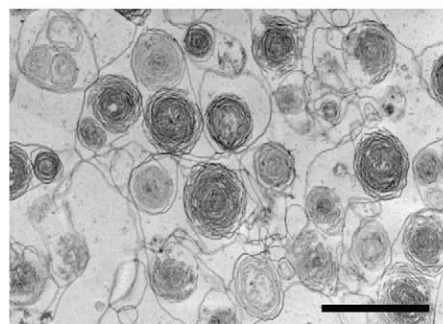
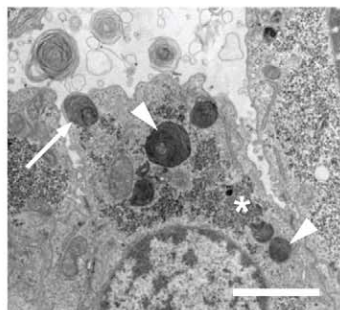
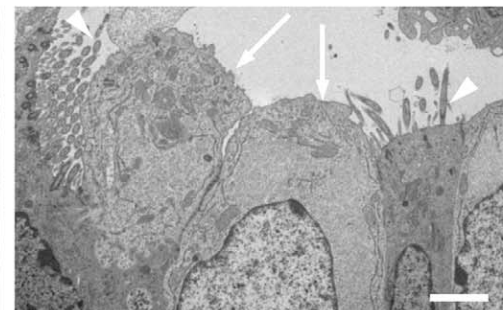
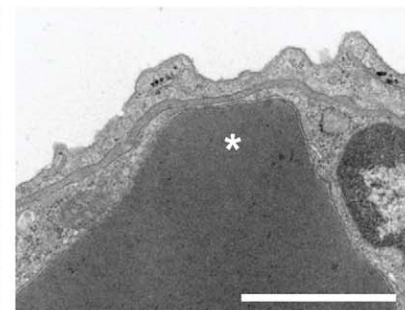
A**B****C****D****E****F****G**

Figure 3. Zfp148 deficiency prevented structural maturation of prenatal lungs without effecting epithelial cell differentiation or surfactant production. (A) Photomicrographs showing lung morphology (hematoxylin and eosin; HE) and glycogen content (periodic acid-Shiff; PAS) and CC10 immunofluorescence in P1 lungs from *Zfp148^{gt/gt}* and wt mice, respectively. (A, B) Graphs show quantification ($n=6$) of mean tissue area per total lung area, PAS-positive area with bronchioles excluded, and CC10-positive area with bronchioles excluded in (A) P1 and (B) E19.5 lungs from wt and *Zfp148^{gt/gt}* mice. a.u., arbitrary units. (C) Real-time RT-PCR showing relative expression levels of markers for type I (T1alpha, Aqp5), type II (Sftpa1, Sftpb, Sftpc, Sftpd), clara (CC-10, Pon1), endothelial (Pecam1, Tie2, Nos3) and smooth muscle (Acta2) cells in *Zfp148^{gt/gt}* lungs compared to wt at P1 ($n=6$). Wt means are represented by the horizontal straight line at 1. (D) Transmission electron microscope (TEM) image of *Zfp148^{gt/gt}* lung at E18.5–19.5 showing lamellar bodies secreted into the lumen of a terminal sac. (E–G) TEM images showing differentiated cells in *Zfp148^{gt/gt}* lungs at E18.5–19.5. (E) Apical part of an alveolar type II cell containing typical lamellar bodies (arrowheads), one of which is in the process of exocytosis (arrow), and accumulations of densely contrasted glycogen particles (asterisk). (F) Two ciliated cells (arrowheads) surrounding two Clara cells (arrows) with bulging appearance and mitochondria accumulated in the apical cytoplasm. (G) High power view of the blood-alveolar barrier showing an erythrocyte (asterisk) in close contact with a highly attenuated part of an endothelial cell that shares a basal lamina with the alveolar type I cell. Scale bars, 2 μ m. * $P<0.05$, *** $P<0.001$.

doi:10.1371/journal.pone.0055720.g003

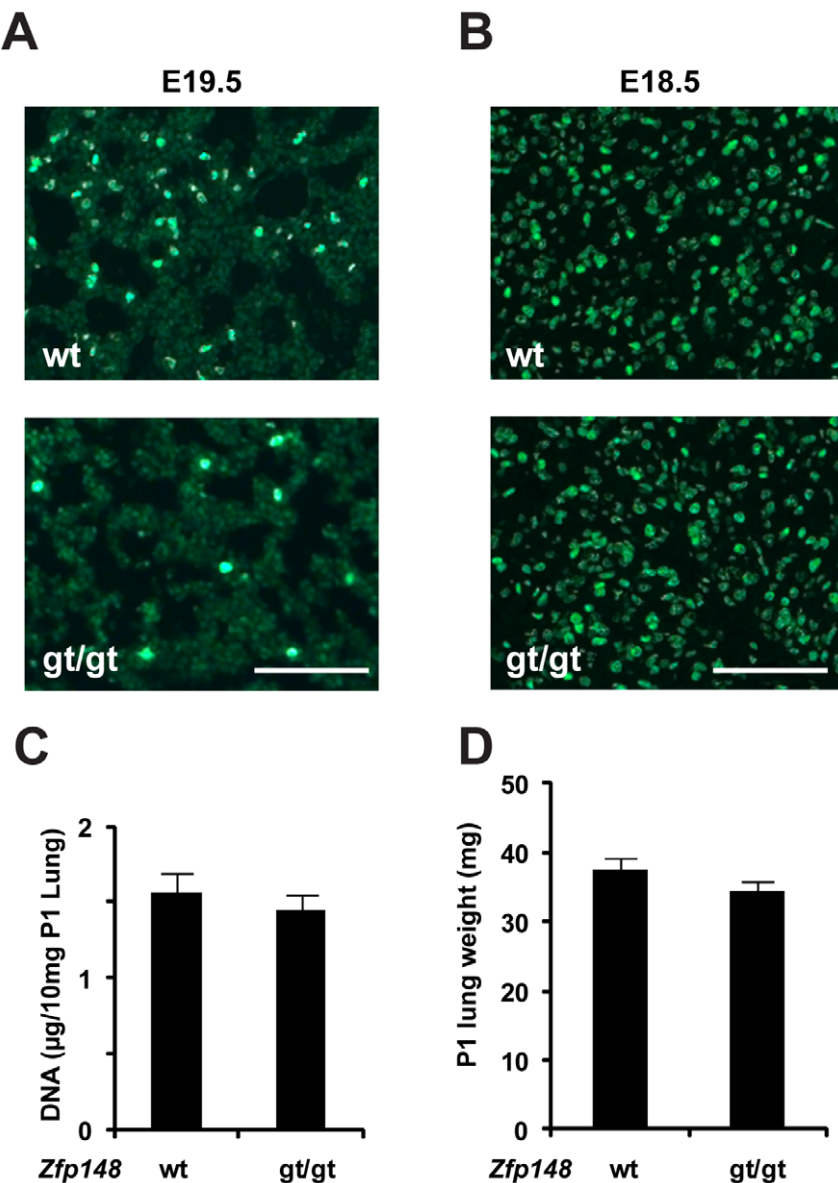


Figure 4. Zfp148 deficiency reduced cell proliferation at the saccular stage of lung development. (A, B) Photomicrographs showing BrdU labeling of E19.5 (A) and E18.5 (B) lungs, respectively, from wt and *Zfp148^{gt/gt}* mice. (C) DNA content per 10 mg lung tissue ($n=5$). (D) Lung wet weight at P1 ($n=12$). Scale bars, 100 μ m.

doi:10.1371/journal.pone.0055720.g004

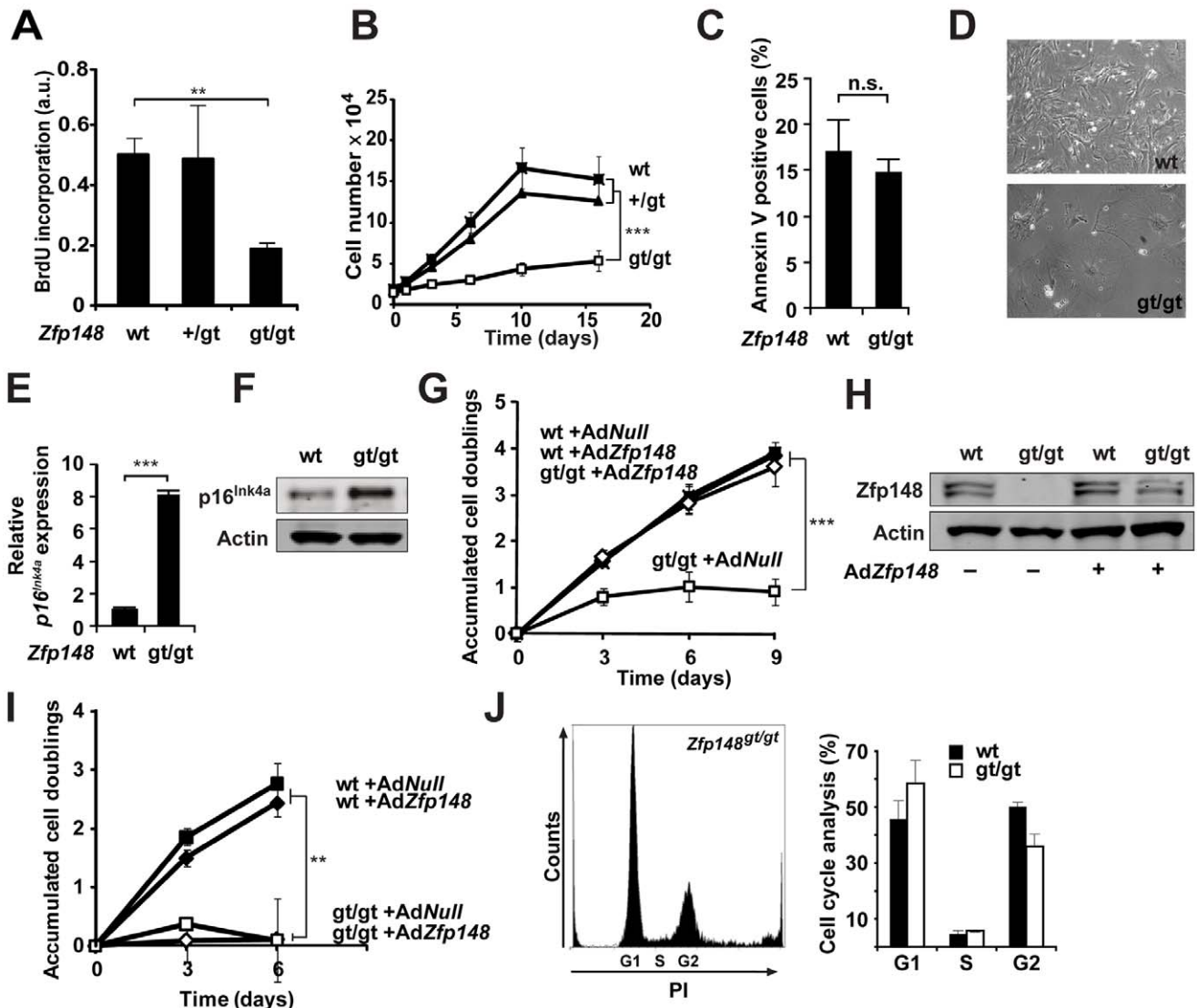


Figure 5. Proliferation arrest in Zfp148^{gt/gt} MEFs. (A) Quantification of BrdU incorporation in wt, Zfp148^{+/gt} and Zfp148^{gt/gt} MEFs ($n=3$). (B) Proliferation of Zfp148^{gt/gt}, Zfp148^{+/gt}, and wt MEFs ($n=4$). (C) Apoptosis defined by FACS analyses of Annexin V in wt and Zfp148^{gt/gt} MEFs at passage 2 ($n=3$). (D) Photomicrographs of wt and Zfp148^{gt/gt} MEFs at passage 2. (E) Real-time RT-PCR of p16^{INK4a} mRNA in wt and Zfp148^{gt/gt} MEFs ($n=4$). (F) Western blot analysis of p16^{INK4a} protein in wt and Zfp148^{gt/gt} MEFs. (G) Cumulative population doublings (CPD) of Zfp148^{gt/gt} and wt MEFs transduced with AdZfp148 or AdNull at passage 0 ($n=3$). (H) Western blot analysis of Zfp148 expression levels in wt and Zfp148^{gt/gt} MEF cell lines transduced with AdZfp148. (I) CPD of Zfp148^{gt/gt} and wt MEFs transduced with AdZfp148 or AdNull at passage 2 ($n=3$). (J) Cell cycle profile of Zfp148^{gt/gt} MEF (left) and quantification of cell cycle distribution of Zfp148^{gt/gt} and wt MEFs ($n=5$) (right) at passage 4 measured by FACS analysis of propidium iodide (PI)-labelled cells. ** $P<0.01$, *** $P<0.001$.

doi:10.1371/journal.pone.0055720.g005

Transmission Electron Microscopy

Lungs were fixed in 2% paraformaldehyde and 2.5% glutaraldehyde. Tissue slices were post-fixed in reduced osmium tetroxide and uranyl acetate, dehydrated, and embedded in epoxy resin. Ultrathin sections (Leica UC6 ultramicrotome) were examined in a LEO 912AB electron microscope.

Surfactant Lipid Analysis

Lipids from lung tissue were extracted as described [20]. Levels of cholesteryl esters, triglycerides and free cholesterol were determined by HPLC [21]. Analysis of phospholipids was performed by mass spectrometry [22].

DNA Synthesis

5-bromo-2'-deoxyuridine (BrdU, Calbiochem/Merck) (20 μ mol/l) was added to the culture medium for 4 h and determined with an ELISA kit (Calbiochem/Merck). For *in vivo* BrdU labelling, pregnant mothers were injected with 150 mg/kg BrdU (Roche), and lungs from E19.5 embryos were collected 2 hours after injection.

Cell Culture

Primary MEFs were isolated from E13.5–14.5 embryos and cell proliferation assays were performed as described [18]. When indicated, the culture medium was supplemented with 100 μ mol l⁻¹ NAC (Sigma Aldrich) and changed daily.

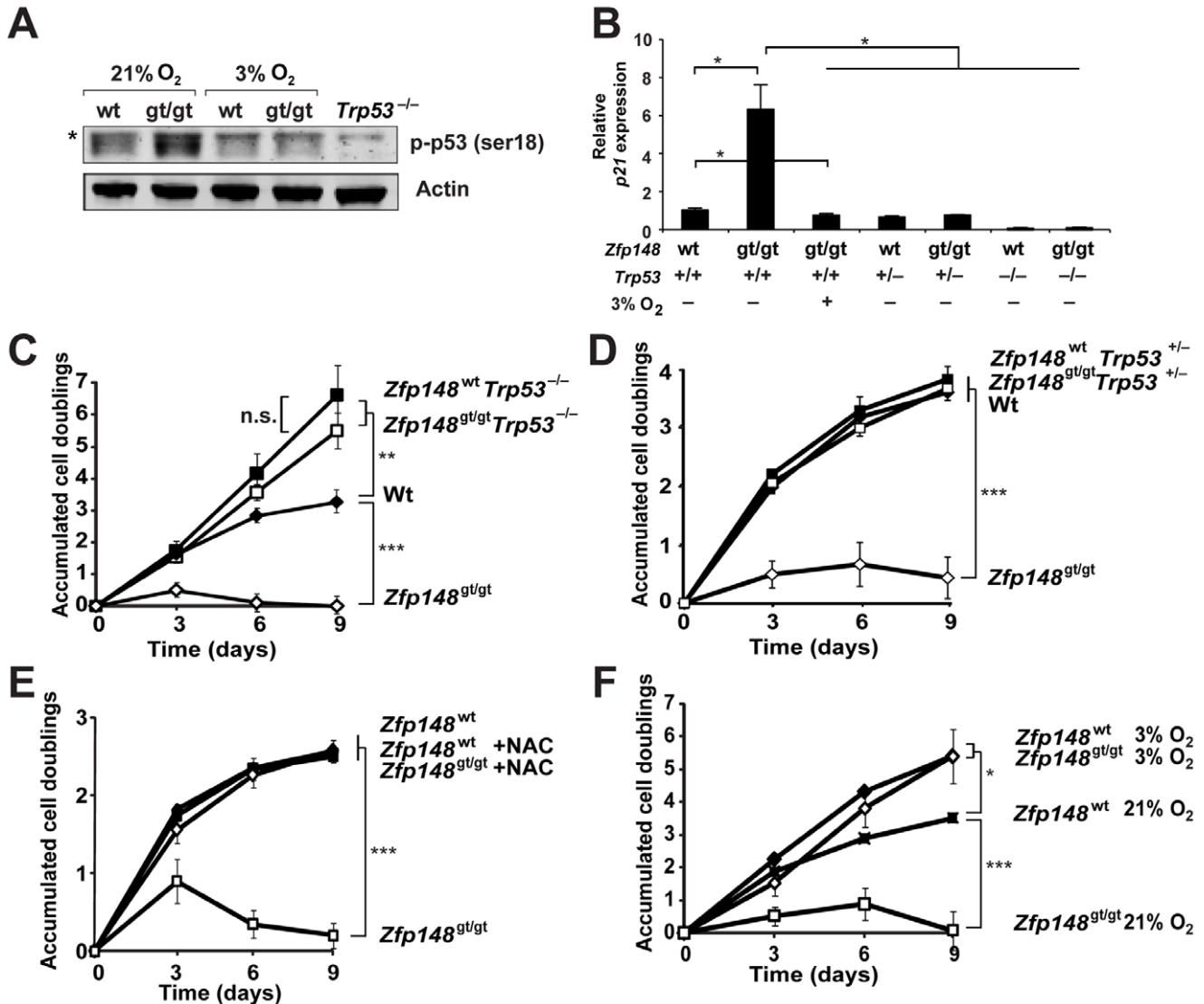


Figure 6. Activation of p53 and *Trp53*-dependent proliferation arrest in *Zfp148*^{gt/gt} MEFs. (A) Western blots of MEF lysates showing expression of phospho-p53^{Ser18} in wt and *Zfp148*^{gt/gt} MEFs cultured at 21 or 3% oxygen, respectively. *Trp53*^{-/-} cells were used as a negative control and actin was used as a loading control. Asterisk indicates unspecific band. (B) Real-time RT-PCR of p21 in wt and *Zfp148*^{gt/gt} MEFs cultured at 21 or 3% oxygen, respectively, and on *Trp53*^{+/+}, *Trp53*^{+/-} and *Trp53*^{-/-} genetic backgrounds ($n=4$). (C, D) CPD of *Zfp148*^{gt/gt} and wt MEFs on *Trp53*^{+/+} or *Trp53*^{-/-} (C) and *Trp53*^{+/+} or *Trp53*^{+/-} (D) genetic backgrounds ($n=3$). (E, F) CPD of *Zfp148*^{gt/gt} and wt MEFs supplemented with n-acetyl-L-cysteine (NAC) (E) in the culture medium ($n=4$), or cultured at atmospheric (21%) or low (3%) oxygen concentrations (F) ($n=3$). * $P<0.05$, ** $P<0.01$, *** $P<0.001$.

doi:10.1371/journal.pone.0055720.g006

Apoptosis

Apoptosis of cultured cells was evaluated with the Annexin V-EGFP Apoptosis Kit (K104–100, Biovision). Apoptosis in P1 lungs was evaluated by immunohistochemical staining with an antibody recognizing cleaved caspase 3 or with the TUNEL kit ApopTag® Fluorescence In Situ Apoptosis Detection Kit (Millipore).

Adenoviral Transduction of MEFs

Cells were incubated with 15 multiplicities of infection of empty control adenoviruses (AdNull) or adenoviruses encoding *Zfp148* (Ad*Zfp148*) or *Zfp148*FLAG (Ad*Zfp148*FLAG) (Vector Biolabs) for 36–48 h before analyses.

Cell-cycle Analysis

Zfp148^{gt/gt} MEFs at passage 4 were trypsinized, fixed in 70% ethanol, incubated with propidium iodide and RNase A for 30 min at 37°C and analyzed in a FACScan flow cytometer with CellQuest Pro software (version 4.0.2, Becton Dickinson).

NAC Treatment

Pregnant females of *Zfp148*^{+/gt} intercrosses were administered NAC in the drinking water at a concentration of 1 g/l.

Statistics

Values are mean \pm SEM. Statistics were performed with two-tailed Student's *t*-test for comparisons between two groups; one-way ANOVA with Tukey's post-hoc test for multiple groups; two-

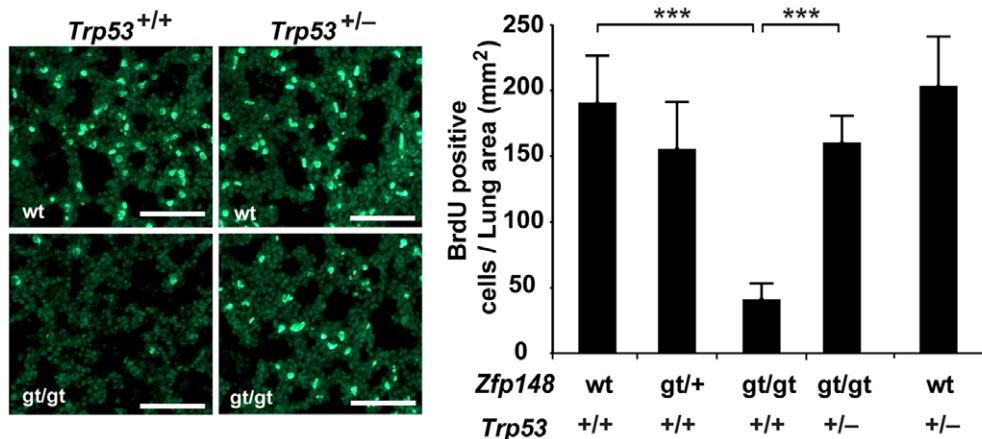
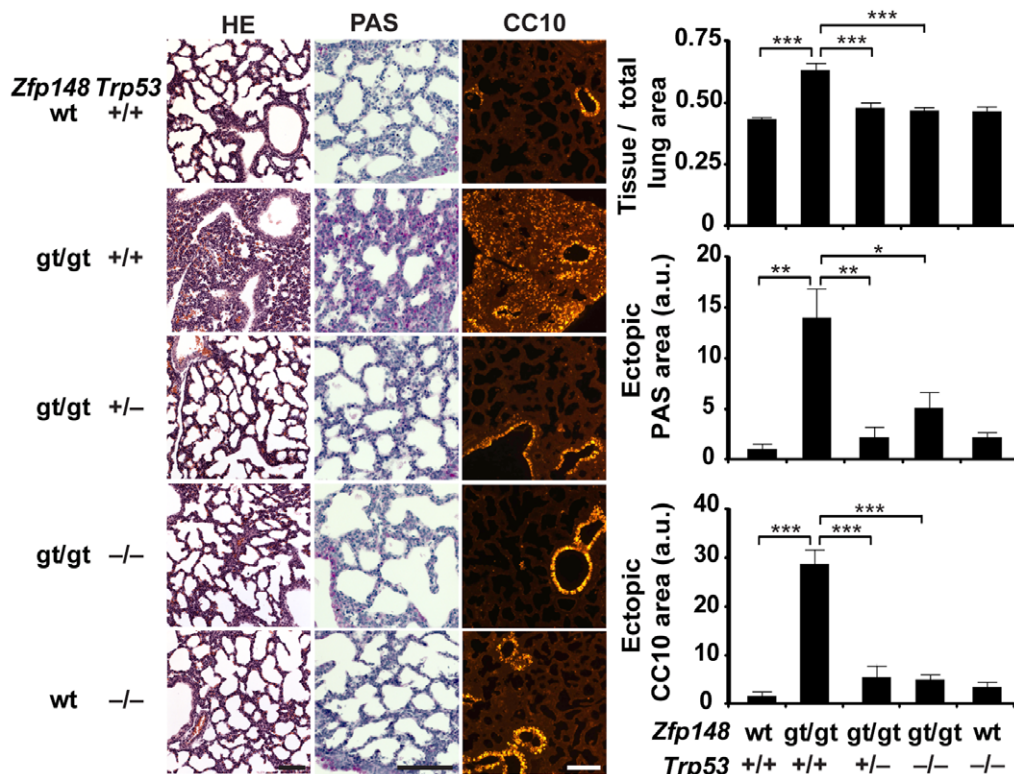
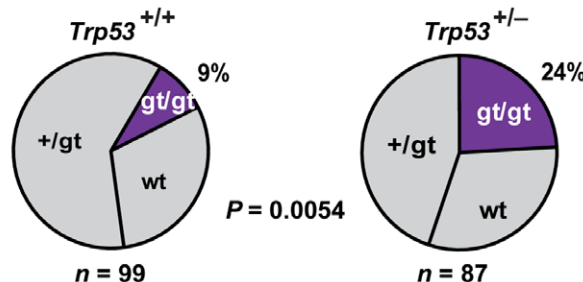
A**B****C**

Figure 7. Deletion of one or two copies of *Trp53* rescued *Zfp148*^{gt/gt} mice from proliferation arrest, respiratory distress and neonatal lethality. (A) Photomicrographs showing BrdU labeling of E19.5 lung from wt, *Zfp148*^{gt/gt}, *Zfp148*^{gt/gt}*Trp53*^{+/-} and *Trp53*^{+/-} mice. Graphs show quantification of BrdU positive cells per lung area (*n*=6 wt, 7 *Zfp148*^{gt/gt}, 7 *Zfp148*^{gt/gt}*Trp53*^{+/-}, 5 *Zfp148*^{gt/gt}*Trp53*^{+/-}, 4 *Trp53*^{+/-}). (B) Photomicrographs showing lung morphology (hematoxylin and eosin; HE) and glycogen content (periodic acid-Schiff; PAS) and CC10 immunofluorescence in P1 lungs from *Zfp148*^{+/+}*Trp53*^{+/+} (*n*=10), *Zfp148*^{gt/gt}*Trp53*^{+/+} (*n*=9), *Zfp148*^{gt/gt}*Trp53*^{+/-} (*n*=9), *Zfp148*^{gt/gt}*Trp53*^{-/-} (*n*=5), and *Zfp148*^{+/+}*Trp53*^{-/-} (*n*=10) mice, respectively. Graphs show quantification of mean tissue area per total lung area, PAS-positive area with bronchioles excluded, and CC10-positive area.

with bronchioles excluded. (C) Distribution of *Zfp148* genotypes of P1 pups of intercrosses between *Zfp148^{+/gt}Trp53^{+/+}* and *Zfp148^{+/gt}Trp53⁺⁻* mice. Scale bars, 100 μ m. * $P<0.05$, ** $P<0.01$, *** $P<0.001$. doi:10.1371/journal.pone.0055720.g007

way ANOVA for multiple groups and genotypes; log-rank test for survival; Chi-square test for genotype frequencies. Differences between groups were considered significant when $P<0.05$.

Results

Generation of *Zfp148*-deficient Mice

To define the *in vivo* and cellular importance of *Zfp148*, we generated *Zfp148*-deficient mice from a gene-trap ES-cell clone. Southern blot analyses and genomic PCR confirmed that the gene-targeting vector had incorporated into the fourth intron of *Zfp148*, thus disrupting 87% of the coding sequence including the DNA binding zinc finger domains (Fig. 1A–C). ES-cells were injected into C57Bl/6 blastocysts to achieve germline transmission of the *Zfp148^{gt/gt}*-allele. Heterozygous intercrosses of *Zfp148^{+/gt}* mice revealed that *Zfp148* mRNA expression was reduced by >95% in *Zfp148^{gt/gt}* tissues and that the protein was undetectable in western blot analyses (Fig. 1D, E). There were no indications of exon

skipping or cryptic splicing (Fig. 1F). The inserted gene-trap vector harbours a promoterless β -Geo reporter, under control of the endogenous *Zfp148* promoter. X-Gal staining of embryonic day 9.5 (E9.5) *Zfp148^{gt/gt}* mice suggested that *Zfp148* is ubiquitously expressed (Fig. 1G, H), in consistency with earlier results [2,4].

Zfp148 Deficiency Leads to Lethality in Newborn Mice, and Growth Retardation and Reduced Lifespan in Adult Mice

Zfp148^{gt/gt} mice were identified at Mendelian ratios throughout embryonic development, but the frequency dropped to half the expected at postnatal day 1 (P1) suggesting that 50% of the mice died shortly after birth (Fig. 2A). *Zfp148^{gt/gt}* mice at postnatal day P1 were pale and cyanotic indicating respiratory problems (Fig. 2B). *Zfp148^{gt/gt}* mice that survived the neonatal crisis were initially normal in size but displayed impaired growth and reduced lifespan (Fig. 2C–F). To specifically assess the postnatal importance of *Zfp148*, mice that were moribund at five weeks of age

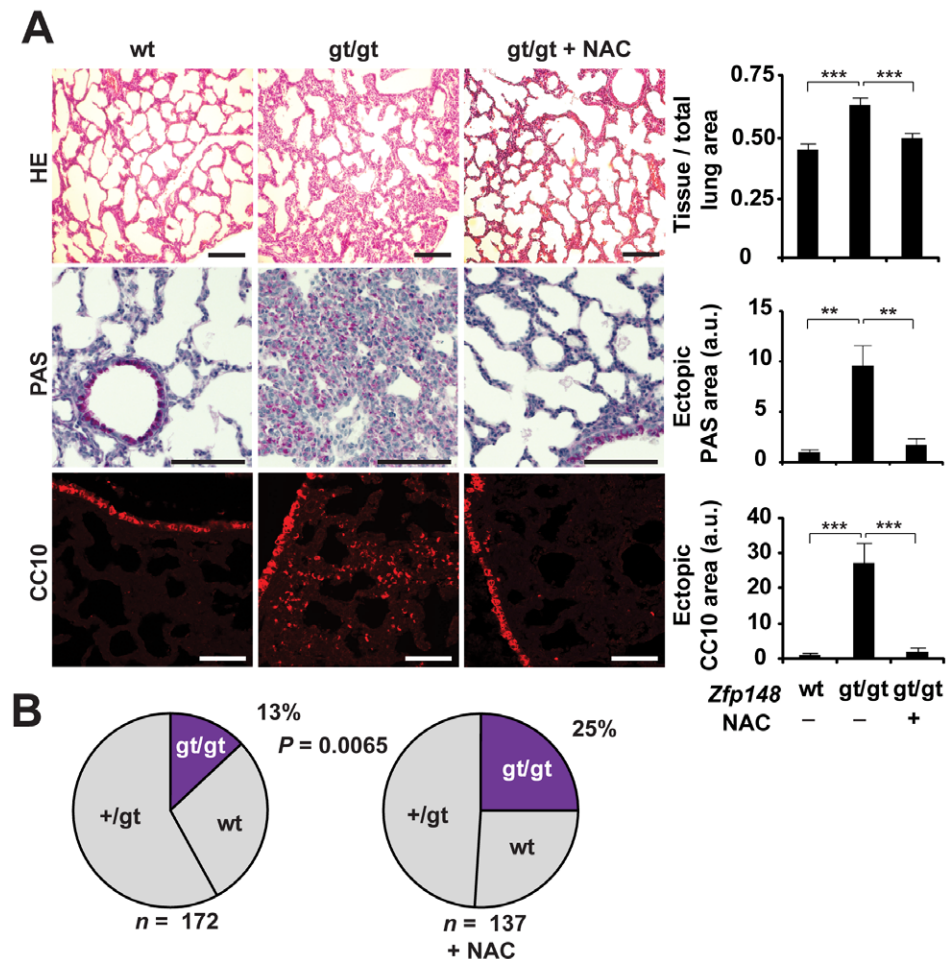


Figure 8. Antioxidant rescue of defect lung maturation and neonatal lethality in *Zfp148^{gt/gt}* mice. (A) Photomicrographs showing lung morphology (hematoxylin and eosin; HE) and glycogen content (periodic acid-Shiff; PAS) and CC10 immunofluorescence in P1 lungs from *Zfp148^{+/+}*, *Zfp148^{gt/gt}*, and NAC treated *Zfp148^{gt/gt}* mice, respectively ($n=6$). Graphs show quantification of mean tissue area per total lung area, PAS-positive area with bronchioles excluded, and CC10-positive area with bronchioles excluded. (B) Distribution of *Zfp148* genotypes of P1 pups of intercrosses between *Zfp148^{+/gt}* mice with and without NAC treatment. Scale bars, 100 μ m. ** $P<0.01$, *** $P<0.001$. doi:10.1371/journal.pone.0055720.g008

(study start) were excluded from the lifespan study. The study is therefore likely to underestimate mortality at young ages.

Respiratory Distress in Newborn *Zfp148^{gt/gt}* Mice is Caused by Defect Lung Maturation

The cyanotic appearance of *Zfp148^{gt/gt}* mice at P1 suggested problems with oxygenation. Histological analyses of lung tissue revealed poorly developed respiratory saccules with thickened primary septae, increased glycogen deposits and widespread ectopic expression of the Clara cell 10 kDa secretory protein CC10 (Fig. 3A). Analyses of lungs at E19.5 revealed that glycogen accumulation and ectopic CC10 expression occurred before birth (Fig. 3B). The results suggest a defect in sacculation, i.e. the transformation of distal lung buds into thin-walled terminal sacs that occurs at E18.5–P5 in mice.

Ectopic expression of CC10 protein indicated that cell differentiation could be disturbed in *Zfp148^{gt/gt}* lungs. However, differentiation of type II cells appeared normal, as judged by the expression of surfactant-related genes, the presence of lamellar bodies, and levels of the surfactant lipid dipalmitoylphosphatidylcholine (Fig. 3C–E; Supporting Information Table S1). There was further no difference in the appearance of blood air barriers or expression of biomarker genes for type I cells (T1alpha, Aqp5) or endothelium (Pecam1, Tie2, Nos3) (Fig 3C, G). Notably, mRNA levels for the Clara cell markers CC10 and Pon1 were slightly reduced in *Zfp148^{gt/gt}* lungs, in spite of the ectopic expression of CC10 protein, indicating that Clara cell differentiation could be affected, although the cells appeared morphologically normal (3C, F). We conclude that *Zfp148* deficiency prevents structural maturation of the prenatal lung without affecting type II cell differentiation or surfactant production.

Zfp148-deficiency Disrupts Cell Proliferation at the Saccular Stage of Lung Development

Zfp148 is implicated in cell cycle control suggesting that *Zfp148^{gt/gt}* lung defects could involve disturbed cell proliferation or apoptosis. To assess if cell proliferation was affected, E18.5 and E19.5 pregnant females were injected with 5-bromo-2'-deoxyuridine (BrdU). *Zfp148^{gt/gt}* lungs at E19.5 contained fewer BrdU-positive cells compared to *Zfp148^{+/gt}* lungs and controls, indicating problems with cell proliferation (Fig. 4A). There was no difference in BrdU incorporation at E18.5 between *Zfp148^{gt/gt}* lungs and controls (Fig. 4B), suggesting that cell proliferation is interrupted during the saccular stage and that defective proliferation is coupled to the maturation defect. In consistency with those results, *Zfp148* deficiency did not affect total lung DNA content or lung wet weight at P1 (Fig. 4C, D), as would have been expected if proliferation was disturbed at earlier stages. There was no difference in apoptosis as judged by staining for activated caspase 3 or the TUNEL assay (Supporting Information Fig. S1).

Zfp148 Deficiency Arrests Cell Proliferation in a Cell Autonomous Manner

To investigate mechanisms underlying the proliferation defect in *Zfp148^{gt/gt}* lungs, mouse embryonic fibroblasts (MEFs) were isolated from E13.5–14.5 embryos of heterozygous intercrosses. *Zfp148^{gt/gt}* MEFs proliferated poorly at early passages (Fig. 5A, B) but did not show increased apoptosis (Fig. 5C), compared to wildtype controls. *Zfp148^{gt/gt}* MEFs exhibited morphological signs of senescence and expressed the senescence marker p16^{ink4a} (Fig. 5D–F), in consistency with a previous study [8]. The proliferation arrest of *Zfp148^{gt/gt}* MEFs was abolished by restoring near physiological expression levels of *Zfp148* by adenoviral

transduction (*AdZfp148*) at passage 0 (Fig. 5G, H). *AdZfp148* transduction at passage 2 did not reverse the proliferation arrest (Fig. 5I), suggesting that cell cycle arrest is irreversible once established. *Zfp148^{gt/gt}* MEFs were arrested regardless of their position in the cell cycle, as judged by cell cycle analysis at passage 4 (Fig. 5J).

Zfp148 Deficiency Lowers the Threshold for p53 Activation and Proliferative Arrest under Oxidative Conditions

Zfp148 deficiency is not likely to arrest cell proliferation under physiological conditions, since *Zfp148^{gt/gt}* embryos develop to term without gross malformations. The tumour suppressor p53 induces proliferative arrest in response to a wide range of stressors, including oxidative stress [23,24]. The interaction of *Zfp148* with p53 opens up for the possibility that *Zfp148* deficiency lowers the threshold for p53-activation. To assess this possibility, levels of phosphorylated p53 were measured under oxidative and non-oxidative conditions. We observed increased levels of phospho-p53^{Ser18} (p53^{Ser15} in humans) protein in *Zfp148^{gt/gt}* MEFs cultured at 21% oxygen, but not at 3% oxygen (Fig. 6A). Similarly, levels of mRNA for the p53-target *p21* were increased in *Zfp148^{gt/gt}* MEFs cultured at 21% oxygen, but not at 3% oxygen (Fig. 6B).

To assess if the proliferation arrest of *Zfp148^{gt/gt}* MEFs is mediated by p53, cells were obtained from *Zfp148^{gt/gt}* mice and controls, bred on a *Trip53* null background. Loss of one or two copies of *Trip53* abolished proliferative arrest in *Zfp148^{gt/gt}* MEFs (Fig. 6C, D and Supporting Information Fig. S2). In line with those results, induction of *p21* was abolished in *Zfp148^{gt/gt}* MEFs on *Trip53^{+/-}* or *Trip53^{-/-}* background (Fig. 6B).

The selective activation of p53 in *Zfp148*-deficient MEFs cultured at 21% oxygen, suggest that oxidative stress is part of the underlying mechanism. To determine if oxidative stress contributes to the proliferative arrest, *Zfp148^{gt/gt}* MEFs were cultured in the presence of the antioxidant *n*-acetyl-L-cysteine (NAC) or at low oxygen concentrations (3%). Both treatments prevented the proliferative arrest (Fig. 6E, F).

Deletion of One or Two Copies of *Trip53* Rescued *Zfp148^{gt/gt}* Mice from Proliferation Arrest, Respiratory Distress and Neonatal Lethality

We further investigated if the proliferation arrest and maturation defect of *Zfp148^{gt/gt}* lungs are mediated by p53. Indeed, loss of one copy of *Trip53* restored cell proliferation in *Zfp148^{gt/gt}* lungs, as judged by BrdU incorporation (Fig. 7A). Moreover, loss of one or two copies of *Trip53* prevented the thickening of the primary septae, glycogen accumulation, and ectopic CC10 expression in *Zfp148^{gt/gt}* lungs (Fig. 7B). The loss of one copy of *Trip53* also rescued *Zfp148^{gt/gt}* mice from neonatal lethality (Fig. 7C).

Antioxidant Rescue of Respiratory Distress and Neonatal Lethality of *Zfp148^{gt/gt}* Mice

To determine if the respiratory distress and neonatal lethality of *Zfp148*-deficient mice are triggered by oxidative stress, we added NAC in the drinking water of pregnant females of heterozygous intercrosses. Strikingly, NAC treatment of pregnant females normalized lung morphology and prevented glycogen accumulation and ectopic CC10 expression of *Zfp148^{gt/gt}* offspring, and rescued them from neonatal death (Fig. 8A, B).

Discussion

In this study, we show that *Zfp148* deficiency in mice causes respiratory distress and neonatal lethality, and that both of those effects were rescued on *Trip53^{+/−}* and *Trip53^{−/−}* genetic backgrounds and by antioxidant treatment. Mechanistic analyses showed that *Zfp148* deficiency lowered the threshold for p53 activation under oxidative conditions thus disrupting cell proliferation and structural maturation of the prenatal lung.

Zfp148 deficiency prevented structural maturation of the prenatal lung without affecting type II cell differentiation or surfactant production. In this respect, *Zfp148*-deficient mice differ from other transgenic models with similar structural maturation defects, since those models also display impaired epithelial cell differentiation or lack of surfactant [25–33]. Thus, *Zfp148* deficiency may unravel novel aspects of lung development.

Our data demonstrate that *Zfp148* deficiency activates p53, and that structural maturation defects in *Zfp148*-deficient lungs are secondary to unchecked p53 activity. The mechanism by which p53 disrupts lung maturation is, however, not clear. Proliferation arrest of pulmonary cells probably contributes to the phenotype, but effects of p53-activation on cytoskeletal remodeling or cell migration, as described in [34–37], may play a role. Effects on cell differentiation are also possible, as judged by the ectopic expression of CC10 and reduced expression of Clara cell biomarker genes. Nevertheless, the rescue of *Zfp148^{gt/gt}* lungs upon deletion of *Trip53* or antioxidant treatment shows that *Zfp148* deficiency affects cell stress or stress responses, whereas *Zfp148* is dispensable for lung development *per se*.

The results show for the first time that *Zfp148* is required for cell proliferation *in vivo*, confirming previous *in vitro* data [8]. Cell proliferation was selectively arrested in prenatal lungs whereas the embryo as a whole developed to term without gross malformations, suggesting that *Zfp148* is required for proliferation in certain contexts. The antioxidant rescue of *Zfp148*-deficient lungs and the rescue on *Trip53^{+/−}* and *Trip53^{−/−}* genetic backgrounds, suggest that the main function of *Zfp148* is to protect cells from p53-activation under oxidative conditions. In consistency with those results, *Zfp148* deficiency lowered the threshold for p53-activation by oxygen in MEFs. Although *Zfp148* deficiency may alter redox homeostasis, the previously demonstrated binding between *Zfp148* and p53 opens up for the possibility that *Zfp148* primarily regulates p53 [14]. Our demonstration of genetic interaction between *Zfp148* and *Trip53* in mice supports this possibility. Formal evidence of the proposed regulation will, however, require generation of *Zfp148* mutants with deficient p53-binding. Future experiments should also establish whether concentrations of reactive oxygen species are elevated in *Zfp148*-deficient cells.

Prenatal lungs are particularly sensitive to the loss of *Zfp148* and tissue hypoxia could be a contributing factor. Hypoxia increases production of reactive nitrogen or oxygen species in the mitochondria thus generating oxidative stress [38–41]. Mice targeted for *Hypoxia-inducible factor 2α* (*Hif2α*), or mice lacking *Hif1a* in airway epithelium, exhibit structural maturation defects reminding of those seen in *Zfp148*-deficient mice with additional effects on epithelial cell differentiation and surfactant production [25,42]. Hypoxia-inducible factors are only active under hypoxic conditions [43,44], suggesting that hypoxia is a driving force of prenatal lung maturation. Thus, levels of reactive nitrogen or oxygen species could be elevated in pulmonary cells at this stage, compared to other cells in the embryo, making them vulnerable to *Zfp148* deficiency.

The defects of *Zfp148*-deficient lungs are reminiscent of clinical findings in newborns with bronchopulmonary dysplasia (BPD).

BPD is a developmental disorder with disrupted postnatal growth of the distal lung caused in part by oxidative damage inflicted by oxygen supplementation of preterm infants [45,46]. Our finding, that *Zfp148* protects the prenatal lung from p53-induced proliferation arrest in response to oxidative stress in mice, opens up for the possibility that *Zfp148* plays a role in the oxidative damage of preterm lungs in BPD. Studies in primates and mice show increased expression of p53 and p21 after postnatal oxygen supplementation [47–49], supporting that possibility.

The physiological role of *Zfp148* has remained uncertain due to inconsistent results of gene targeting experiments in mice. A previous attempt to target *Zfp148* resulted in sterile chimeric mice and it was suggested that haploinsufficiency for *Zfp148* blocks germ cell differentiation [13]. Our study clearly demonstrates that *Zfp148*-heterozygous mice are fertile and that *Zfp148* is dispensable for early mouse development. One possible explanation for this discrepancy is that the targeting strategy used by Takeuchi and co-workers (deletion of exon 9) generates a dominant negative phenotype. Alternatively, the *129P2/OlaHsd* embryonic stem cell line that we used is more robust and maintains pluripotency better upon *Zfp148* deficiency, compared to the *AB1* strain used in Takeuchi's study. We conclude that in the current study, *Zfp148* mRNA levels in *Zfp148^{gt/gt}* cells were reduced by >95% and the *Zfp148* protein was undetectable.

Another study showed that mice generated from the same *Zfp148* gene-trap mutation used in our study die at E8.5–E10.5 with unclosed neural tubes and anaemia [12]. We observed this phenotype in embryos of the first generation (F1) intercrosses. Importantly, this phenotype co-segregated with a gene-trap vector but not with the recombined *Zfp148* locus (Supporting Information Fig. S3A–C). Moreover, the gene-trap vector was propagated to 79% of the brown offspring (F1 mice) of crosses between chimeric mice and C57Bl/6 mice. This deviates from the expected Mendelian distribution (62 of 78 mice, $P=1.5 \times 10^{-7}$, binomial distribution) but is consistent with a second integration of the gene-trap vector in the embryonic stem cell line. Thus, the embryonic death is not caused by *Zfp148* deficiency.

In summary, we show that *Zfp148* is required for structural maturation of the prenatal lung by preventing oxidative stress-dependent p53 activity during the saccular stage of lung development. The result demonstrates for the first time that *Zfp148* plays a critical role for cell cycle progression *in vivo*, and establishes *Zfp148* as a novel factor in mammalian lung development.

Supporting Information

Figure S1 Respiratory distress in *Zfp148*-deficient mice is not caused by apoptosis. TUNEL and cleaved caspase 3 (cl-CASP3) staining in lungs of P1 *Zfp148^{gt/gt}* and wt mice ($n=6$). Sections of thymus from a 3-week-old wild-type mouse were used as a positive control. (TIF)

Figure S2 Wt and *Zfp148*-deficient MEF proliferation on *Trp53^{+/−}* or *Trp53^{−/−}* backgrounds ($n=3$). (TIF)

Figure S3 Integration of a second gene-trap in the XB878 ES cell clone. (A) Dissection of 21 E9.5 embryos of F1 generation intercrosses identified a proportion of embryos with unclosed neural tubes and variable degrees of additional defects similar to those described in [12]. Importantly, these mice had at least one intact *Zfp148* allele as judged by PCR-amplification of a DNA fragment spanning the gene-trap insertion site of the *Zfp148*

locus (*Zfp148*wt PCR). Moreover, the gene-trap vector was propagated to 79% of the brown offspring (F1 mice) of crosses between chimeric mice and C57Bl/6 mice, which deviates from the expected Mendelian distribution (62 of 78 mice, $P=1.5 \times 10^{-7}$, binomial distribution) but is consistent with the presence of two gene-trap alleles in the injected ES-cells. **(B, C)** Dorsal view of E9.5 embryos exhibiting unclosed neural tubes (arrows). (TIF)

Table S1 HPLC and mass spec analysis of surfactant lipids from P1 lungs from wt and *Zfp148*^{gt/gt} mice, first two columns are means for respective genotypes (n=4) followed by p-value.

(PDF)

References

- Merchant JL, Iyer GR, Taylor BR, Kitchen JR, Mortensen ER, et al. (1996) ZBP-89, a Kruppel-like zinc finger protein, inhibits epidermal growth factor induction of the gastrin promoter. *Mol Cell Biol* 16: 6644–6653.
- Wang Y, Kobori JA, Hood L (1993) The ht beta gene encodes a novel CACCC box-binding protein that regulates T-cell receptor gene expression. *Mol Cell Biol* 13: 5691–5701.
- Hasegawa T, Takeuchi A, Miyaishi O, Isobe K, de Crombrugge B (1997) Cloning and characterization of a transcription factor that binds to the proximal promoters of the two mouse type I collagen genes. *J Biol Chem* 272: 4915–4923.
- Passantino R, Antona V, Barbieri G, Rubino P, Melchionna R, et al. (1998) Negative regulation of beta enolase gene transcription in embryonic muscle is dependent upon a zinc finger factor that binds to the G-rich box within the muscle-specific enhancer. *J Biol Chem* 273: 484–494.
- Bai L, Merchant JL (2000) Transcription factor ZBP-89 cooperates with histone acetyltransferase p300 during butyrate activation of p21waf1 transcription in human cells. *J Biol Chem* 275: 30725–30733.
- Bai L, Kao JY, Law DJ, Merchant JL (2006) Recruitment of ataxiatelangiectasia mutated to the p21(waf1) promoter by ZBP-89 plays a role in mucosal protection. *Gastroenterology* 131: 841–852.
- Wu Y, Zhang X, Salmon M, Zehner ZE (2007) The zinc finger repressor, ZBP-89, recruits histone deacetylase 1 to repress vimentin gene expression. *Genes Cells* 12: 905–918.
- Feng Y, Wang X, Xu L, Pan H, Zhu S, et al. (2009) The transcription factor ZBP-89 suppresses p16 expression through a histone modification mechanism to affect cell senescence. *FEBS J* 276: 4197–4206.
- Bai L, Logsdon C, Merchant JL (2002) Regulation of epithelial cell growth by ZBP-89: potential relevance in pancreatic cancer. *Int J Gastrointest Cancer* 31: 79–88.
- To AK, Chen GG, Chan UP, Ye C, Yun JP, et al. (2011) ZBP-89 enhances Bak expression and causes apoptosis in hepatocellular carcinoma cells. *Biochim Biophys Acta* 1813: 222–230.
- Law DJ, Labut EM, Adams RD, Merchant JL (2006) An isoform of ZBP-89 predisposes the colon to colitis. *Nucleic Acids Res* 34: 1342–1350.
- Woo AJ, Moran TB, Schindler YL, Choe SK, Langer NB, et al. (2008) Identification of ZBP-89 as a novel GATA-1-associated transcription factor involved in megakaryocytic and erythroid development. *Mol Cell Biol* 28: 2675–2689.
- Takeuchi A, Mishina Y, Miyaishi O, Kojima E, Hasegawa T, et al. (2003) Heterozygosity with respect to *Zfp148* causes complete loss of fetal germ cells during mouse embryogenesis. *Nat Genet* 33: 172–176.
- Bai L, Merchant JL (2001) ZBP-89 promotes growth arrest through stabilization of p53. *Mol Cell Biol* 21: 4670–4683.
- Bai L, Merchant JL (2007) ATM phosphorylates ZBP-89 at Ser202 to potentiate p21waf1 induction by butyrate. *Biochem Biophys Res Commun* 359: 817–821.
- Law DJ, Labut EM, Merchant JL (2006) Intestinal overexpression of ZNF148 suppresses ApcMin/+ neoplasia. *Mamm Genome* 17: 999–1004.
- Larsson E, Fredlund Fuchs P, Heldin J, Barkefors I, Bondjers C, et al. (2009) Discovery of microvascular miRNAs using public gene expression data: miR-145 is expressed in pericytes and is a regulator of Fli1. *Genome Med* 1: 108.
- Liu M, Sjogren AK, Karlsson C, Ibrahim MX, Andersson KM, et al. (2010) Targeting the protein prenyltransferases efficiently reduces tumor development in mice with K-RAS-induced lung cancer. *Proc Natl Acad Sci U S A* 107: 6471–6476.
- Wasteson P, Johansson BR, Jukkola T, Breuer S, Akyurek LM, et al. (2008) Developmental origin of smooth muscle cells in the descending aorta in mice. *Development* 135: 1823–1832.
- Folch J, Lees M, Sloane Stanley GH (1957) A simple method for the isolation and purification of total lipides from animal tissues. *J Biol Chem* 226: 497–509.
- Homan R, Anderson MK (1998) Rapid separation and quantitation of combined neutral and polar lipid classes by high-performance liquid chromatography and evaporative light-scattering mass detection. *J Chromatogr B Biomed Sci Appl* 708: 21–26.
- Ejsing CS, Duchoslav E, Sampaio J, Simons K, Bonner R, et al. (2006) Automated identification and quantification of glycerophospholipid molecular species by multiple precursor ion scanning. *Anal Chem* 78: 6202–6214.
- Vogelstein B, Lane D, Levine AJ (2000) Surfing the p53 network. *Nature* 408: 307–310.
- Vousden KH, Lane DP (2007) p53 in health and disease. *Nat Rev Mol Cell Biol* 8: 275–283.
- Compernelle V, Brusselmans K, Acker T, Hoet P, Tjwa M, et al. (2002) Loss of HIF-2alpha and inhibition of VEGF impair fetal lung maturation, whereas treatment with VEGF prevents fatal respiratory distress in premature mice. *Nat Med* 8: 702–710.
- Wan H, Luo F, Wert SE, Zhang L, Xu Y, et al. (2008) Kruppel-like factor 5 is required for perinatal lung morphogenesis and function. *Development* 135: 2563–2572.
- Kalin TV, Wang IC, Meliton L, Zhang Y, Wert SE, et al. (2008) Forkhead Box m1 transcription factor is required for perinatal lung function. *Proc Natl Acad Sci U S A* 105: 19330–19335.
- Martis PC, Whitsett JA, Xu Y, Perl AK, Wan H, et al. (2006) C/EBPalpha is required for lung maturation at birth. *Development* 133: 1155–1164.
- Dave V, Childs T, Xu Y, Ikegami M, Besnard V, et al. (2006) Calcineurin/Nfat signaling is required for perinatal lung maturation and function. *J Clin Invest* 116: 2597–2609.
- Wan H, Xu Y, Ikegami M, Stahlman MT, Kaestner KH, et al. (2004) Foxa2 is required for transition to air breathing at birth. *Proc Natl Acad Sci U S A* 101: 14449–14454.
- Grad I, McKee TA, Ludwig SM, Hoyle GW, Ruiz P, et al. (2006) The Hsp90 cochaperone p23 is essential for perinatal survival. *Mol Cell Biol* 26: 8976–8983.
- Yamazaki D, Komazaki S, Nakanishi H, Mishima A, Nishi M, et al. (2009) Essential role of the TRIC-B channel in Ca2+ handling of alveolar epithelial cells and in perinatal lung maturation. *Development* 136: 2355–2361.
- Bridges JP, Lin S, Ikegami M, Shannon JM (2012) Conditional hypoxia inducible factor-1alpha induction in embryonic pulmonary epithelium impairs maturation and augments lymphangiogenesis. *Dev Biol* 362: 24–41.
- Guo F, Gao Y, Wang L, Zheng Y (2003) p19Arf-p53 tumor suppressor pathway regulates cell motility by suppression of phosphoinositide 3-kinase and Rac1 GTPase activities. *J Biol Chem* 278: 14414–14419.
- Guo F, Zheng Y (2004) Rho family GTPases cooperate with p53 deletion to promote primary mouse embryonic fibroblast cell invasion. *Oncogene* 23: 5577–5585.
- Gadea G, Lapasset L, Gauthier-Rouviere C, Roux P (2002) Regulation of Cdc42-mediated morphological effects: a novel function for p53. *EMBO J* 21: 2373–2382.
- Gadea G, Roger L, Anguille C, de Toledo M, Gire V, et al. (2004) TNFalpha induces sequential activation of Cdc42- and p38/p53-dependent pathways that antagonistically regulate filopodia formation. *J Cell Sci* 117: 6355–6364.
- Dirmeyer R, O'Brien KM, Engle M, Dodd A, Spears E, et al. (2002) Exposure of yeast cells to anoxia induces transient oxidative stress. Implications for the induction of hypoxic genes. *J Biol Chem* 277: 34773–34784.
- Chandel NS, Budinger GR (2007) The cellular basis for diverse responses to oxygen. *Free Radic Biol Med* 42: 165–174.
- Guzy RD, Hoyos B, Robin E, Chen H, Liu L, et al. (2005) Mitochondrial complex III is required for hypoxia-induced ROS production and cellular oxygen sensing. *Cell Metab* 1: 401–408.
- Poyton RO, Ball KA, Castello PR (2009) Mitochondrial generation of free radicals and hypoxic signaling. *Trends Endocrinol Metab* 20: 332–340.
- Saini Y, Harkema JR, LaPres JE (2008) HIF1alpha is essential for normal intrauterine differentiation of alveolar epithelium and surfactant production in the newborn lung of mice. *J Biol Chem* 283: 33650–33657.
- Jaakkola P, Mole DR, Tian YM, Wilson MI, Gilbert J, et al. (2001) Targeting of HIF-alpha to the von Hippel-Lindau ubiquitylation complex by O2-regulated prolyl hydroxylation. *Science* 292: 468–472.
- Kaelin WG, Jr., Ratcliffe PJ (2008) Oxygen sensing by metazoans: the central role of the HIF hydroxylase pathway. *Mol Cell* 30: 393–402.

Table S2 Primer List.
(PDF)

Acknowledgments

We thank Christer Betsholtz, Fredrik Backhed, Ulf Lindahl, Jonas Nilsson, and Anne Uv for helpful discussions and Rosie Perkins for comments on the manuscript.

Author Contributions

Conceived and designed the experiments: VIS PL. Performed the experiments: VIS AN MXI PA EL MP LMH MS BRJ. Analyzed the data: VIS AN MXI EL MS BRJ MOB PL. Wrote the paper: VIS MOB PL.

45. Kinsella JP, Greenough A, Abman SH (2006) Bronchopulmonary dysplasia. *Lancet* 367: 1421–1431.
46. Baraldi E, Filippone M (2007) Chronic lung disease after premature birth. *N Engl J Med* 357: 1946–1955.
47. Maniscalco WM, Watkins RH, Roper JM, Staversky R, O'Reilly MA (2005) Hyperoxic ventilated premature baboons have increased p53, oxidant DNA damage and decreased VEGF expression. *Pediatr Res* 58: 549–556.
48. Das KC, Ravi D, Holland W (2004) Increased apoptosis and expression of p21 and p53 in premature infant baboon model of bronchopulmonary dysplasia. *Antioxid Redox Signal* 6: 109–116.
49. Londhe VA, Sundar IK, Lopez B, Maisonet TM, Yu Y, et al. (2011) Hyperoxia impairs alveolar formation and induces senescence through decreased histone deacetylase activity and up-regulation of p21 in neonatal mouse lung. *Pediatr Res* 69: 371–377.